WELDING RESEARCH

SUPPLEMENT TO THE *WELDING JOURNAL*, SEPTEMBER 1992

Sponsored by the American Welding Society and the Welding Research Council

Determination of Residual Stresses in Thick-Section Weldments

The time and cost of analyzing stresses in a thick multipass weldment are reduced with the use of a reliable numerical model

BY Y. SHIM, Z. FENG, S. LEE, D. KIM, J. JAEGER, J. C. PAPRITAN AND C. L. TSAI

ABSTRACT. The purpose of this study is to develop an analytical method for predicting through thickness distribution of residual stresses in a thick plate with a multipass welding process. The analysis was carried out in two steps. The first step was to develop a thermal model for heat flow analysis in a two-dimensional cross-section of the plate. For a modeling of the heat input to the cross-section, a ramp heat input was used to avoid numerical instability and to include the effect of a moving arc. The best ramp time was selected by an analysis of the root pass on a ½-in. (12.7-mm) thick plate and comparing it with experiments.

The next step was to develop a structural model to predict stress distribution using the thermal loading obtained in the first step. A generalized plane strain assumption was used in the stress analysis. A lumped pass model was developed to reduce the total computational time and cost. Each layer of weld bead was assumed as one lumped pass in this model. The heat input for every pass in that layer was added and applied on the top surface of a weld layer. The results by the lumped model showed good agreement with the experiment and the results of another model, which analyzed every weld pass separately.

Y. SHIM, Z. FENG, S. LEE, D. KIM, J. JAEGER, J. C. PAPRITAN and C. L. TSAI are with The Ohio State University, Columbus, Ohio.

Introduction

Residual stress is developed as a result of manufacturing and fabricating a steel structure. It can be a major factor for cracking and fracture problems in heavy structures (Ref. 1). In welded structures, nonlinear thermal loading cycles are created by a welding arc. This thermally induced loading produces nonlinear thermal strains which result in residual stresses after welding. There are practical difficulties in measuring through thickness residual stresses, because through thickness stress measurement techniques are destructive and require lots of time. Therefore, numerical analysis is a very effective method in predicting residual stress distribution through the thickness.

KEY WORDS

Residual Stresses
Thick-Section Weldment
Thick Plate
Thermal Model
Heat Flow Analysis
2-D Model
Structural Model
Stress Distribution
Structural Welding
Multipass Welds

As the plate thickness increases, the number of weld passes required for a complete joint penetration weld also increases. Consequently, the plate is subjected to more complex thermal cycles and more complex inelastic strain patterns. Currently, little data are available pertaining to the magnitude and nature of residual stresses in multipass welding, especially in the through thickness direction. As the plate thickness increases, the number of weld passes also increases, which requires a longer computational time to determine stresses. Therefore, it is necessary to develop an analytical model to reduce the computational time. The objective of this study is to develop a numerical evaluation methodology for thermal and residual stress fields created by welding of thick plates and to verify the results experimentally.

The thermal and stress responses of weldments are three-dimensional problems that may require a considerable

Pass Sequence	Pass No.	Welding Parameters		
		Current (A)	Voltage (V)	Speed (IPM)
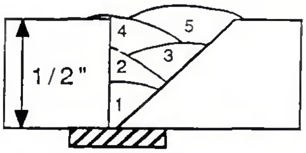	1	215	24	14.4
	2	205	25	14.4
	3	215	26	14.4
	4 - 5	210	24	14.4
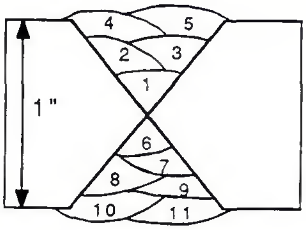	1	190	25	7.9
	2 - 5	215	26	11.1
	6	190	25	7.9
	7 - 9	220	26	11.1
	10 - 11	250	27	11.1
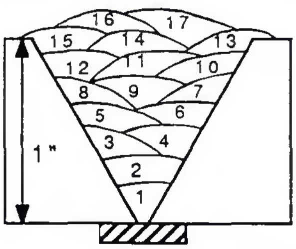	1 - 2	195	24.5	6.6
	3 - 6	200	24.5	7.9
	7 - 12	190	24.5	7.9
	13	195	24.5	7.9
	14 - 17	190	24.8	6.6

Fig. 1 — Schematics of pass sequences along with welding parameters for each pass.

amount of computing time and cost. Therefore, it is almost impossible to analyze multipass welding in a thick plate with three-dimensional modeling. Frequently, symmetry along the cross-section is assumed to reduce the problem to a two-dimensional plane strain analysis. Adequate results with the plane strain assumption have been reported by many investigators (Refs. 2, 3). In multipass welding of thick plates with a free boundary condition, plane strain assumptions may not adequately represent the constraint along the welding direction. A generalized plane strain assumption was implemented in this study to consider the strain of the cross-section in the welding direction. Many commercial finite element packages have been successfully employed in the analysis of welding problems (Refs. 2, 4). This study was performed with the help of ABAQUS, a commercial finite element analysis package (Ref. 5).

Temperature profiles were obtained through the use of thermocouples and a data-acquisition system developed at the Department of Welding Engineering, Ohio State University (Ref. 6). Residual stresses at the surface of the plates were measured using the blind-hole drilling method. The plates were annealed before welding to minimize the influence of pre-existing stress from prior cutting or rolling. The experimental temperature fields and residual stresses were compared with finite element results.

Experiment

The experimental tests were directed toward collecting temperature and stress information on the surface of the weldments. The experimental results were used for a comparison and verification of the finite element model.

The data-acquisition system was designed to measure the temperature and strain changes during welding. It was also developed to monitor strain relaxation during blind-hole drilling for a residual stress measurement. It was composed of four major components: an IBM AT computer, an HP3497A data-acquisition/control unit, an IBM graphic printer, and an HP6214B power supply. The overall maximum speed of the system was about ten channels per second. Generally, this speed was fast enough for monitoring the temperature changes and the strain changes during welding.

Thermocouples were used to record the surface temperature changes during welding. Quantitative data at certain locations were collected via thermocouples for a local comparison with the finite element results. Surface temperatures were measured on ½-in. (12.7-mm) and 1-in. (25.4-mm) thick plates using ANSI Type K thermocouples. All thermocouples were mounted around the middle of the transverse cross-section of the specimens.

The blind-hole drilling method was used to experimentally determine the surface residual stresses in the weldment (Refs. 7, 8). The strain gauges used were designed and manufactured for the blind-hole drilling method by Measurement Group, Inc. (gauge pattern: EA-06-062RE-120). A high-speed air turbine drill was used to reduce the drilling-induced stress. The strain relaxation data used to convert strains to residual stresses were those taken when the hole depth reached 1.2 times the hole diameter, as recommended by the strain gauge manufacturer. To obtain accurate blind-hole drilling results which reflect only the residual stress from welding, the drilling must be performed slowly with minimal pressure, otherwise additional thermal and mechanical strains from drilling will be superimposed. To achieve this goal, the drilling process usually took approximately six minutes to complete. Residual stress measurements were obtained at locations around the middle transverse cross-section of the specimens.

The test specimens were prepared using a ASTM A36 plate. A single bevel butt joint was prepared for the ½-in.-thick plate, and both single- and double-V-grooves were prepared for the 1-in.-thick plate. Pass sequences and welding parameters are shown in Fig. 1. In order to remove pre-existing residual stresses, the 1-in.-thick plate was stress relieve annealed prior to welding. Thermocouples were attached after locally polishing the surface of the specimens.

A GMAW system and BUG-O automatic traveling unit were combined to make an automatic process system. To accurately measure heat input, a voltmeter and ampere meter were attached to the welding system. An E70S-3-type electrode was used. The shielding gas was composed of 98% Ar - 2% O_2.

Finite Element Model

Thermal Model

The material properties used in this research were from ASTM A36 mild

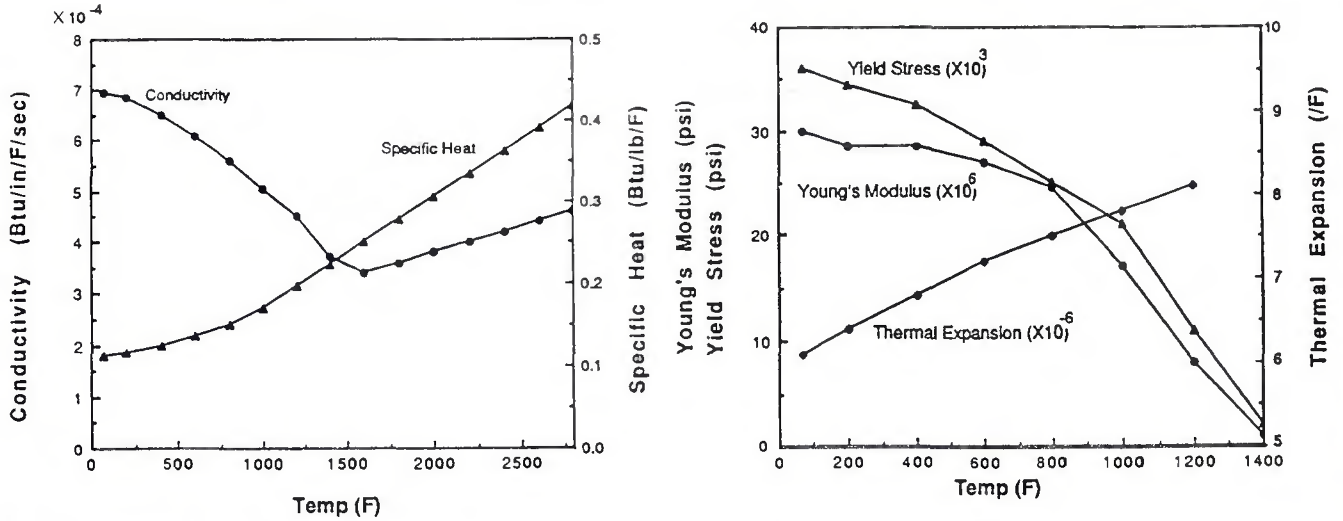

Fig. 2 — Temperature-dependent material properties.

steel. The temperature-dependent thermal and mechanical properties are shown in Fig. 2 (Ref. 9).

In this study, symmetry along the cross-section was assumed to reduce the problem to a two-dimensional analysis, where heat flow was limited to a cross-section perpendicular to the welding direction, with an assumption of steady-state conditions. Since plastic deformation has a negligible effect on the welding temperature field, an uncoupled thermomechanical analysis was performed. This implies that the thermal analysis was initially performed, and the temperature history from that analysis was used as the loading input for the subsequent stress analysis. The finite element mesh and time steps were identical for both the heat flow analysis and the stress analysis.

The size of the finite element mesh has a great effect on the accuracy of the results and computational cost. The trade off between mesh size and computational cost must be considered. From previous experience (Ref. 10), the element size used for the weld area was smaller than or equal to the depth of the weld bead. Since a butt joint welded plate was symmetric about the weld line, only one half of the plate was modeled. A two-dimensional finite element mesh shown in Fig. 3 was used for both the heat transfer and stress analysis. The area with oblique lines represents layers of weld bead. It was determined from the actual weld bead shown in Fig. 1. Eight-node rectangular elements were used for both thermal and stress analysis.

The fusion zone mesh was stair-stepped to numerically represent the individual weld beads. Elements representing each weld bead were initially removed and activated for each pass to simulate a deposition of the weld beads. A heat flux was applied to these newly activated elements to generate a heat input. The size of the time increments used was dependent on the magnitude of the temperature gradients. The maximum allowable temperature change between time increments was limited to 200°F (111°C). The temperature data for each time increment were saved as input to the stress analysis. An arc efficiency of 85% was used for a net heat input to the plate.

A heat flux was applied to the model gradually by using a ramp heat input model that was developed to allow variable ramp times. The ramp heat input model was developed to avoid numerical convergence problems due to an instantaneous increase in temperature near the fusion zone and to include the effect of a moving arc in the two-dimensional plane. A general amplitude-time curve shape for the ramp input model is

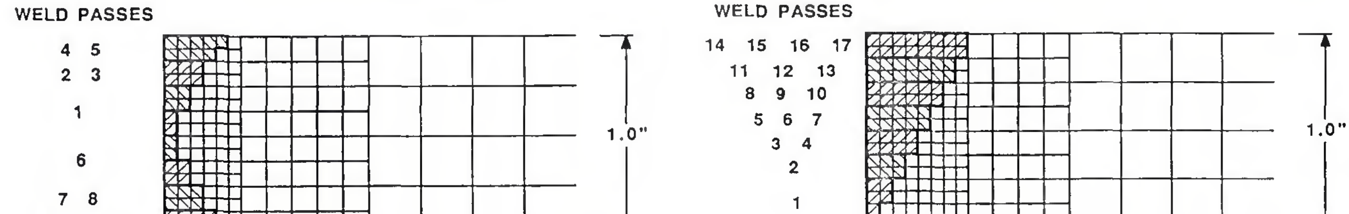

Fig. 3 — Clockwise from top left: Finite element mesh for ½-in.-thick plate; finite element mesh for 1-in.-thick plate with a double V-groove; finite element mesh for 1-in.-thick plate with a single V-groove ; finite element mesh for 2-in.-thick plate.

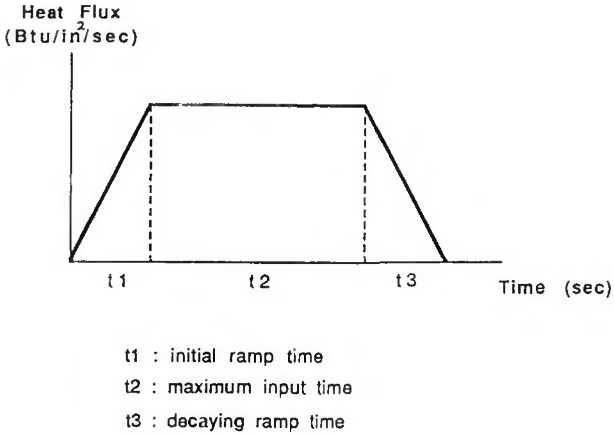

Fig. 4 — Numerical model of heat flux input.

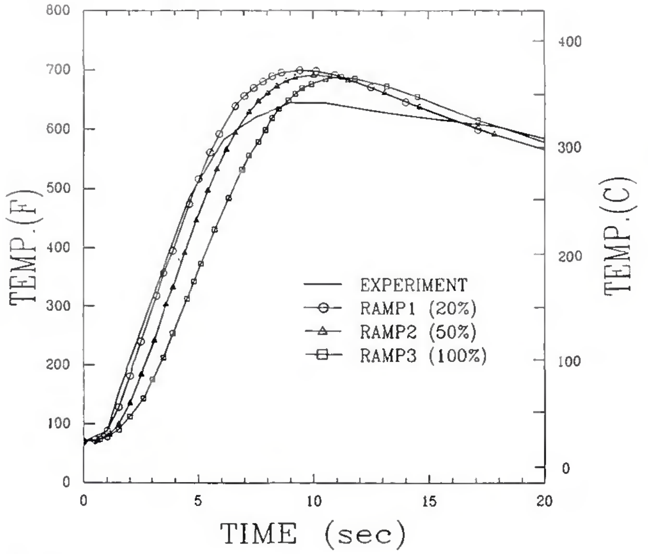

Fig. 5 — Effect of ramp times for the first pass of ½-in.-thick plate (¼ in. from centerline at the top).

shown in Fig. 4. It shows the variation of heat flux with time. The total welding time for the arc to travel across a unit thickness of the finite element model was t1+t2. Ramp times (t1 and t3) from 10 to 100% of the total actual heat input time (t1+t2) were considered in the study of ramp time effect. The total area under these various ramp heat curves was kept constant to insure that the same total heat input to the model was maintained.

The thermal analysis temperature history results for the ½-in.-thick plate were compared with the experimental data to achieve the best ramp heat input model. Figure 5 shows the temperature profiles at ¼ in. (6.4 mm) from the joint edge preparation for the first pass of the ½-in.-thick plate with various ramp heat input models. The general trend was for larger ramp times to decrease peak temperatures and cooling rates. The temperature profiles for large ramp times were shifted to the right indicating more time was required to reach a peak temperature. The maximum difference in times to reach a peak temperature was about 2 s. The maximum temperature difference during the heating cycle was about 180°F (100°C). The temperature difference during the cooling cycle was very small compared with the heating cycle. Numerical temperature profiles were also compared with experimental data at ½ in. from the edge preparation at the top surface of the plate as shown in Fig. 6. General trends were the same as the temperature profiles at ¼ in. (6.4 mm) from the edge, but the effect of ramp time was less dominating as the distance from the edge increased. Generally, a ramp time of 20% of the total weld time (t1+t2) gave the best correlation with the experimental data. Consequently, this value was used for the temperature analysis of 1-in. and 2-in. (50.8-mm) thick plates.

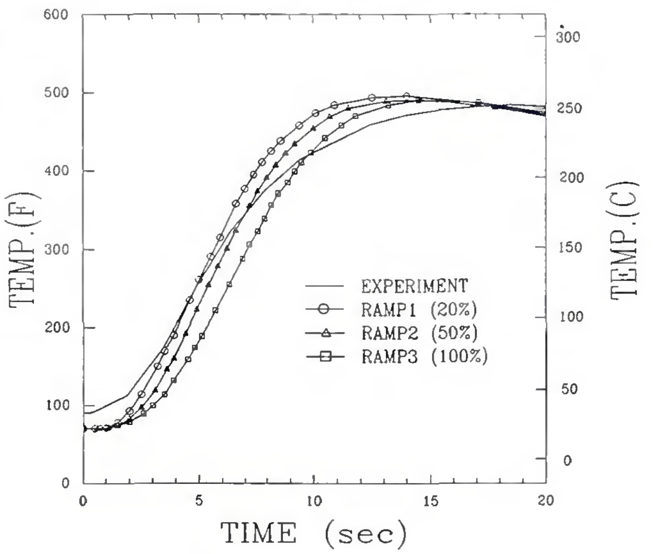

Fig. 6 — Effect of ramp times for the first pass of ½-in.-thick plate (½ in. from centerline at the top).

Mechanical Model

A generalized plane strain theory was used for the stress analysis to consider the strain of the cross-section in the direction of welding (Ref. 11). The generalized plane strain theory assumed that the model between two initially parallel planes in the thickness direction may move as rigid bodies with respect to each other, so strains vary linearly throughout the cross-section. The same finite element mesh and time increments were used for both the thermal and structural analysis.

The fusion zone elements were incrementally activated to model the weld passes as they were deposited. The temperature history obtained from the thermal analysis was input as a thermal loading into the structural model to calculate thermal strains and stresses for each time increment. These thermal strains and stresses were accumulated to produce the final state of residual stresses.

Free boundary conditions were used for the free surfaces except at the centerline of the cross-section, where a symmetry condition was used. Volume changes due to phase transformations were neglected. Initial stresses and strains were zero, since the test specimens were stress relaxed before welding. The mass of the plate was not included in the analysis, which was negligible compared to thermal stresses.

Two models were used for the stress analysis of 1- and 2-in. thick plates. The first model assumed a heat flux of an individual pass, and was distributed over the top surface of one layer of weld bead.

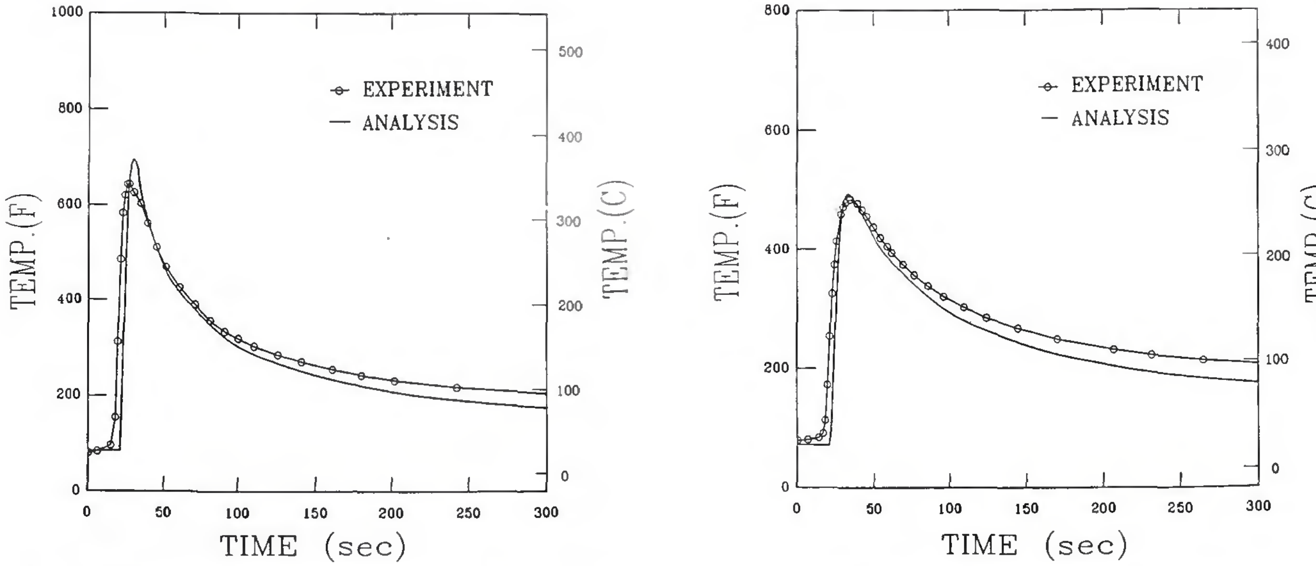

Fig. 7 — Left: Temperature profiles for the first pass of ½-in.-thick plate (¼ in. from centerline at the top); right: temperature profiles for the first pass of ½-in.-thick plate (½ in. from centerline at the top).

The result of temperature analysis for each pass was used as thermal loading in the stress analysis. Analysis was repeated for each pass needed to complete one layer. The second model (lumped model) used lumped passes. Each layer of weld bead was considered as one lumped pass in this model. Heat fluxes for each pass in that layer were added and distributed over the top surface of the layer. This is a very efficient method for reducing the computational cost for both thermal and stress analysis, especially for thick plates. A total of 11 passes were lumped into 6 passes in 1-in.-thick plate with a double V-groove, 17 passes were lumped into 7 passes in 1-in.-thick plate with a single V-groove, and 32 passes were lumped into 14 passes in 2-in.-thick plate with a double V-groove. The results of stress analysis for both models were compared with experimental data.

Results and Discussion

Thermal Analysis

Figure 7 shows the numerically calculated temperature vs. time plots for the first pass of the ½-in.-thick plate at ¼ and ½ in. from the centerline on the top surface. Experimental results from the thermocouples were also plotted for a comparison. The temperature profiles from the analysis showed good correlation with the experimental data near the weld. This is important since high temperature in this area usually results in large plastic strains and thermal stresses. Generally, the differences between the peak temperatures calculated by the thermal analysis and the experimental results were less than 50°F (28°C) (±10%). A ramp time consisting of 20% of the total heat input time was used, which was determined from the study of a ramp time effect.

Figure 8 shows the temperature profiles for the first pass of the 1-in.-thick plate with a double V-groove at a ½ in. and a ¾ in. (19.1 mm) from the centerline on the top surface. The maximum difference in the peak temperature between two results was less than 70°F (39°C). The results showed similar trends as in the ½-in.-thick plate. Each pass modeled in the thermal analysis was divided

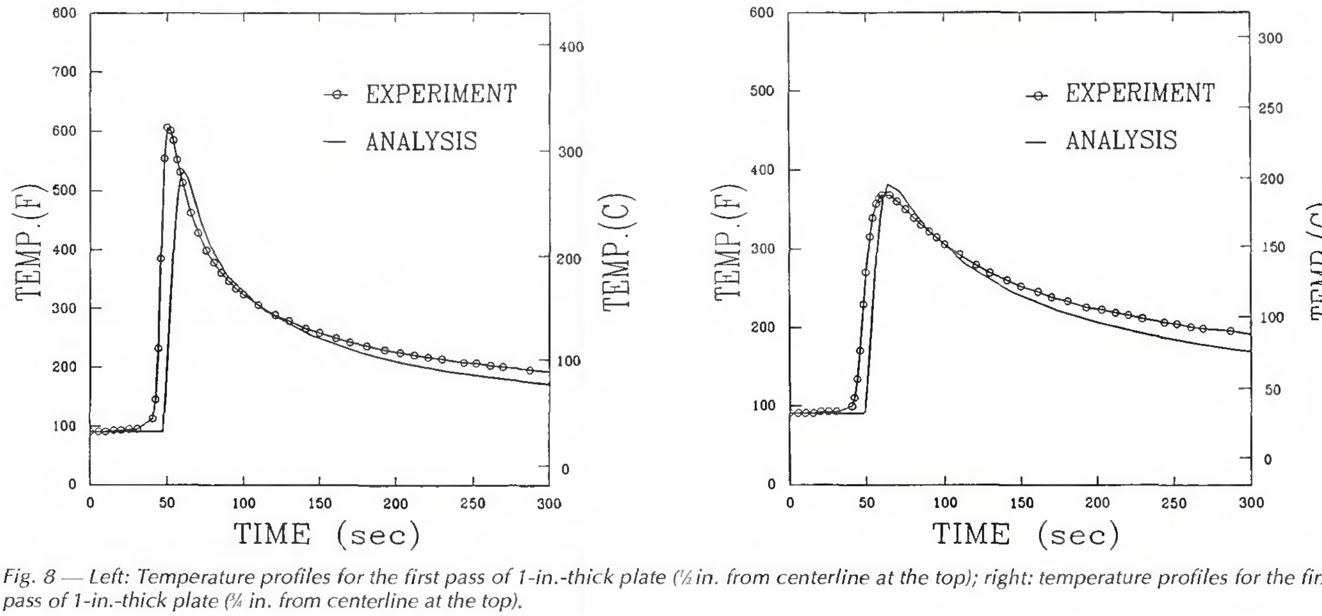

Fig. 8 — Left: Temperature profiles for the first pass of 1-in.-thick plate (½ in. from centerline at the top); right: temperature profiles for the first pass of 1-in.-thick plate (¾ in. from centerline at the top).

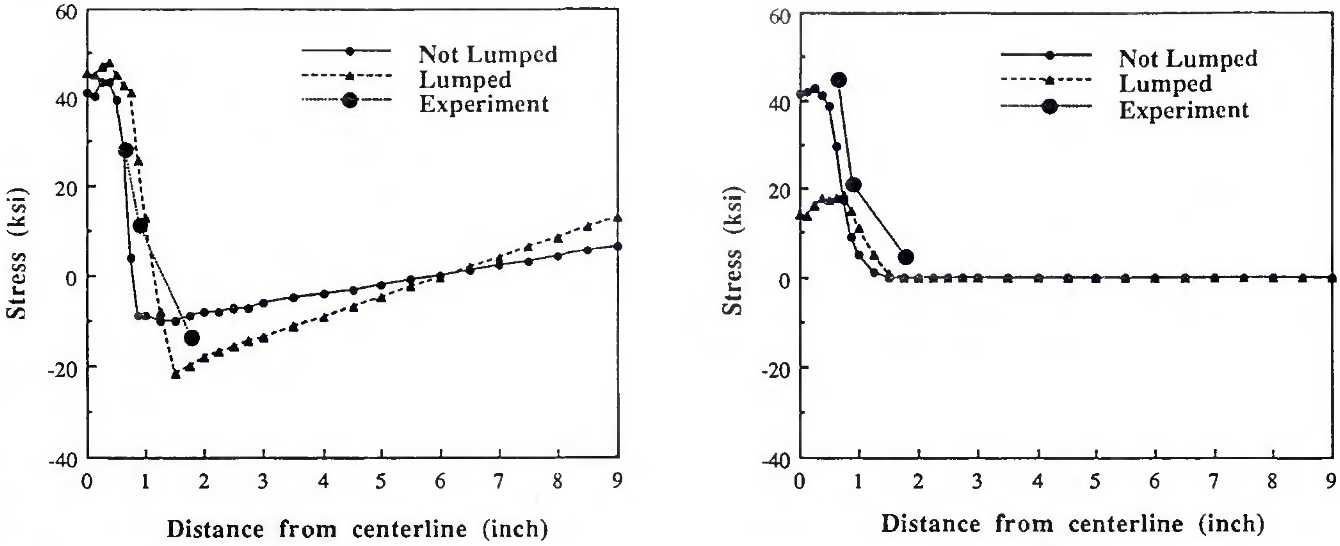

Fig. 9 — Left: Longitudinal stress at the top surface of 1-in.-thick plate with a double V-groove; right: transverse stress at the top surface of 1-in.-thick plate with a double V-groove.

into small time increments, such that the maximum temperature change between any two time increments was less than 200°F (111°C). The temperature data for each increment were saved and used as a thermal loading to the stress analysis.

Stress Analysis

Figure 9 shows the longitudinal (welding direction) and transverse (perpendicular to welding direction) stresses at the top surface of the 1-in.-thick plate with a double V-groove. The first model (not-lumped) analyzed every welding pass. The heat flux was distributed over one layer of weld bead. The second model (lumped) used lumped passes. A total of 11 passes were lumped into 6 passes. The results of both analysis were compared with experimental data. Both results show tensile yield stress around the weld centerline, but the tensile zone was increased by about ⅓ in. (8.5 mm) in the lumped model. The lumped model showed higher longitudinal compressive stress outside the weld area than the not-lumped model. Generally, experimental data fall between two analytical results in a longitudinal stress distribution. The first model (not-lumped) showed higher tensile transverse stress around the weld centerline than the lumped model. Experimental results showed good agreement with the first model.

Figure 10 shows the longitudinal and transverse stresses at the top surface of the 1-in.-thick plate with a single V-groove. Seventeen passes were reduced to 7 lumped passes in the lumped model. The lumped model showed slightly lower tensile longitudinal stress around the weld centerline. Longitudinal tensile stress zone was increased by about ½ in. in the lumped model. Transverse stresses were also reduced and the tensile zone was increased in the lumped model. General trends were similar to the results of 1-in.-thick plate with a double V-groove.

The longitudinal and transverse stresses at the top surface of the 2-in.-thick plate with a double V-groove are shown in Fig. 11. Thirty-two passes were reduced to 14 passes in the lumped model. The maximum stress difference in the two models was less than 10 ksi (69 MPa) and longitudinal tensile stress zone was increased by about ½ in. in the

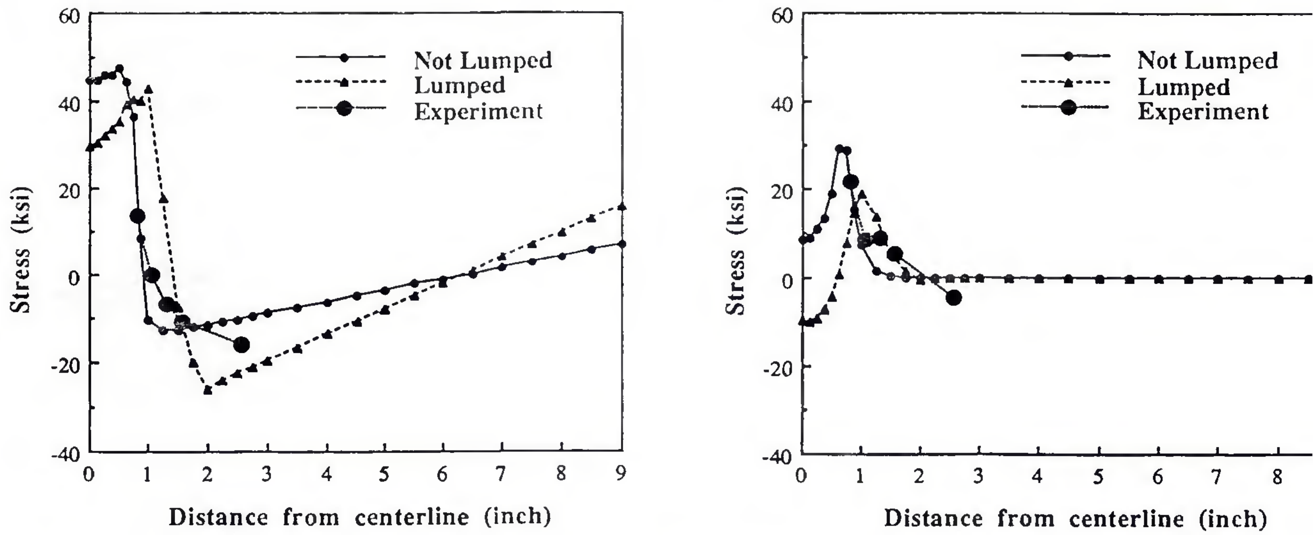

Fig. 10 — Left: Longitudinal stress at the top surface of 1-in.-thick plate with a single V groove; right: transverse stress at the top surface of 1-in.-thick plate with a single V-groove.

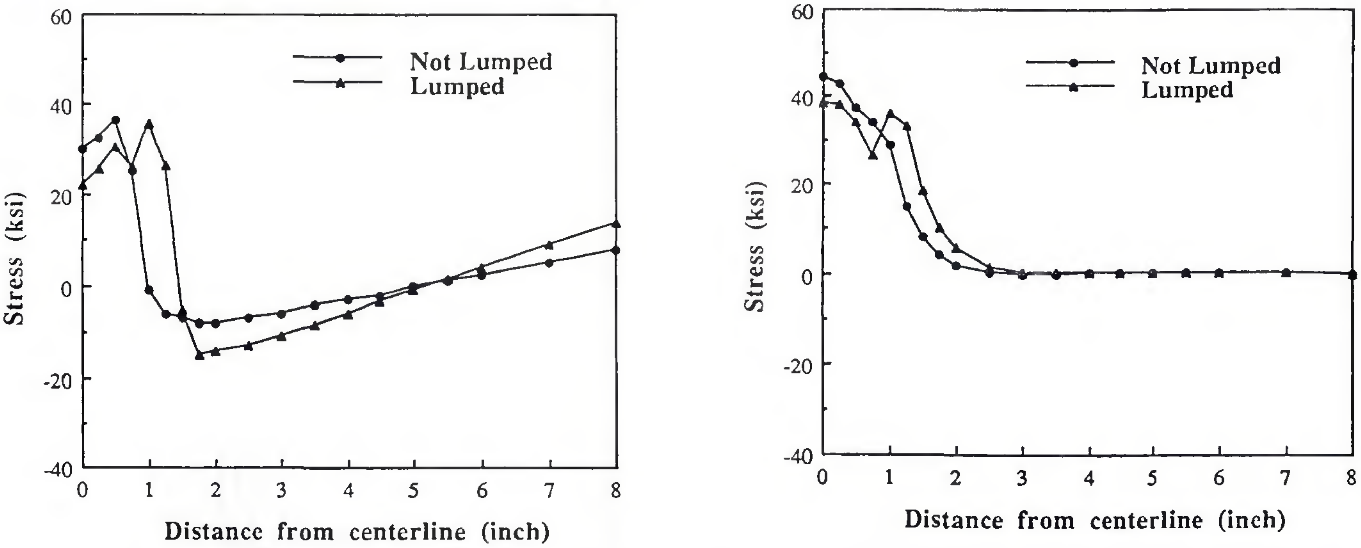

Fig. 11 — Left: Longitudinal stress at the top surface of 2-in.-thick plate with a double V-groove; right: transverse stress at the top surface of 2-in.-thick plate with a double V-groove.

lumped model. General trends were similar to the 1-in.-thick plates, but tensile zones were increased compared to the 1-in.-thick plates.

The good agreement between theoretical analysis and experimental results for both transverse and longitudinal stresses built confidence in the application of the generalized plane strain theory to the calculation of residual stresses in multipass weldments. Also, the stress distributions of the lumped model showed very close results to the not-lumped model. Thus, we could use the lumped model with reasonable results of stresses in thick plates.

Figure 12 shows the longitudinal and transverse stress variations at the weld centerline through the thickness of the 2-in.-thick plate with a double V-groove. As shown in the figure, the lumped model showed lower tensile longitudinal stress through the thickness than the first model. The tensile transverse stress at both surface areas was balanced by compressive stress in the middle of the plate. Both transverse and longitudinal stress distributions showed a similar shape. The maximum tensile stress existed near the surfaces of the plate and was gradually decreased at the middle of the plate.

Conclusions

The finite element method was used to analyze temperature and residual stress field in a plate with multipass welding. The results were compared with experimental data containing temperature and residual stress. A ramp heat input was used to include the effect of a moving arc. Various ramp times were studied in the first pass of ½-in.-thick plate. The results of this study showed that 20% of the actual heat input time gave the best correlation with the experiments, and it was used for the rest of the analysis.

A generalized plane strain assumption gave reasonable stress distribution in both longitudinal and transverse directions, which was confirmed by experimental data. The lumped-pass model was developed to reduce computational cost. Each layer of weld bead was considered as one lumped pass. The result was compared with another model that analyzed every weld pass individually. The result of the analysis using the

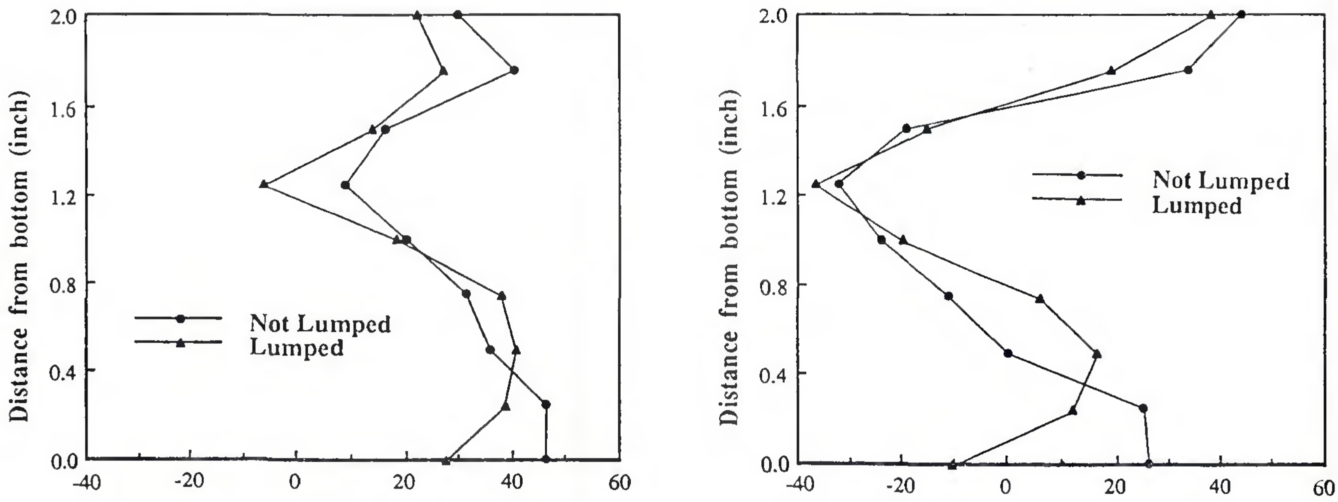

Fig. 12 — Left: Longitudinal through thickness stress for 2-in.-thick plate with a double V-groove at weld centerline; right: transverse through thickness stress for 2-in.-thick plate with a double V-groove at weld centerline.

lumped model showed reliable data compared with both not-lumped model and experimental data.

The effect of joint geometry on the residual stress distribution was studied for 1-in.-thick plate with two different grooves: a single V-groove and a double V-groove. The results showed that the joint geometry was not a sensitive parameter as far as residual stress was concerned.

The stress field through the thickness was investigated and showed that the maximum stress existed near the surface. The longitudinal stress showed high-tensile stress through the thickness, but the transverse stress changed from tensile stress at the surface to compression near the middle of the thickness.

Acknowledgment

The authors acknowledge and appreciate the support of the U.S. Army Corps of Engineers for this project.

References

1. Finite Element Modeling of Welded Thick Plates for Bonneville Navigation Lock. Project Report. The Ohio State University, Department of Welding Engineering. 1990.

2. Free, J. A., and Porter Goff, R. F. D. 1989. Predicting residual stress in multipass weldments with the finite element method. Computer & Structures, 32(2): 365–378.

3. Argyris, J. H., Szimmat, J., and William, K. J. 1982. Computational aspects of welding stress analysis. *Computer Methods in Applied Mechanics and Engineering* 33: 635–666.

4. Tekriwal, P., Stitt, M., and Mazumder, J. 1987. Finite element modeling of heat transfer for gas tungsten arc welding. *Metal Construction*, Oct., pp. 599R–606R.

5. ABAQUS User's Manual, HKS Co., 1989.

6. Determination of residual stress and effects in thick section weldments for hydraulic structures. Project Report. The Ohio State University, Department of Welding Engineering. 1990.

7. *Determining Residual Stresses by the Hole-Drilling Strain Gage Method.* ASTM Standard E837-85.

8. Measurement of residual stresses by the blind hole drilling method. TN-503. Measurement Group, Inc., 1988.

9. *Metals Handbook.*.ASM International 1948.

10. Boyles, L. G., Lee, W. C., and Kim, D. S. 1987. Weld joint analysis for CIT vacuum chamber. Final report to GA Technologies.

11. *ABAQUS Theory Manual*, HHS Co., 1989.

WRC Bulletin 362
April 1991

Recommended Practices in Elevated-Temperature Design: A Compendium of Breeder Reactor Experiences (1970–1987), Volume I—Current Status and Future Directions

Edited by A. K. Dhalla

The recommended practices for elevated-temperature design of liquid metal fast breeder reactors (LMFBR) have been consolidated into four volumes to be published in four individual WRC bulletins.

Volume I: Current Status and Future Directions (WRC Bulletin 362)
Volume II: Preliminary Design and Simplified Methods (WRC Bulletin (363)
Volume III: Inelastic Analysis (WRC Bulletin 365)
Volume IV: Special Topics (WRC Bulletin 366)

Volume I presents the current status of the international design codes and structural technology for LMFBR's. Structural components designed by various countries that were found to be successful for long-term elevated-temperature operation are included.

Publication of this bulletin was sponsored by the Committee on Elevated Temperature Design of the Pressure Vessel Research Council. The price of WRC Bulletin 362 is $45.00 per copy, plus $5.00 for U.S. and $10.00 for overseas, postage and handling. Orders should be sent with payment to the Welding Research Council, Room 1301, 345 E. 47th St., New York, NY 10017.